Study of the Mechanical Properties of Bones Under Fracture Healing Conditions with Specific Medical Treatments, Using 4 Point Bending Tests and Ultra-Micro Indentation Techniques

Soraya Diego[1], Estela Ruiz[1], José A. Casado[1], Diego Ferreño[1], Manuel Redondo[1], María I. Pérez[2], José A. Riancho[2], Isidro Carrascal[1], Claudia Demian[1], Federico Gutiérrez-Solana[1] and Christopher Vilupillai[1]

[1] Department of Materials Science University of Cantabria. 39005 Santander (Cantabria). Spain
[2] Universitary Hospital Marqués de Valdecilla. Avda. Valdecilla s/n, 39008 Santander (Cantabria), Spain
* Corresponding author: jose.casado@unican.es

Abstract This paper aims to compare the effectiveness of two medical treatments in healing an induced pseudoarthrosis (bone fracture without direct contact thus driving a callus formation) on the right femurs of Sprague Dawley laboratory rats. To further understand and quantify the mechanical effects of each treatment, the bone mechanical properties were analysed in terms of the following parameters: hardness and elastic modulus using ultra-micro indentation tests, and maximum force, energy absorbed up to maximum force and rigidity using four point bending tests.

To assess the effectiveness of the treatments in terms of mechanical performance, the results were compared against a control group and a regular bone fracture (direct contact between broken bone parts without a gap). Both treatments were successful in restoring properties similar to the control group in terms of overall hardness (in both cortical and trabecular bone tissues) and rigidity. However, one of them appears to provide higher values of maximum force, energy absorbed and bone hardness.

The results provide information that can be extrapolated to further understand the treatment of human bone fractures in terms of mechanical properties. The data enables the comparison of the outcomes that both treatments have on the biomechanical functioning of bone fractures.

Keywords pseudoarthrosis, four point bending test, ultra-micro indentation test, osseous callus

1. Introduction

Since the 1990s, several studies have been trying to transfer engineering methods to analyze biological materials [1-5]. This gave rise to one of the fundamental principles of biomechanics: the reaction of a tissue of an organism to stimuli, obeys the same laws that govern the behavior of typical “engineering” materials. Thus making applicable the methods used to measure engineering material properties to biological tissues, such as bones for example. In order to understand human bone tissues it is usual to study animal bones, as they provide an ideal biomechanical model due to their size and rudimentary functioning, simplifying the analysis of mechanical properties.

This paper compares the effectiveness of two medical treatments, “A” and “B”, on a subtraction osteotomy of Sprague Dawley rat femurs against a control group and a normal fracture. The aim of the paper is to study the effect of “A” and “B” on the healing of a subtraction osteotomy, by applying methods used for calculating engineering material properties. This investigation is complemented with other studies about biological parameters which haven´t been finished yet; for this reason it is necessary to maintain the confidentiality of the name of the treatments considered until the whole study is completed. Results were acquired through 4 point bending tests on the bone sample shafts (diaphysis) and ultra-micro indentation tests on the bone sample extremities (lower and upper extremities). The 4PBTs provided maximum force, energy absorbed up to maximum force and rigidity. The UMI tests enabled the determination of the cortical and trabecular bone hardness and elastic modulus. The data were obtained by using the left and right femurs of twelve

rats, collected in three separate occurrences once every 12 weeks. Due to the biological nature of the material, variations in the results are substantial, even between samples that have undergone identical treatments.

Assessing the effectiveness of “A” and “B” on the fracture healing of rat bones is important, as it supplies information on the viability of using such treatments for humans. Sprague Dawley rats were used because of their similarity to humans in reaction to diseases. This report provides the mechanical properties of the bones for each treatment. If a treatment is successful in providing the bone with feasible parameters, it can then be further investigated for potential human use. Although, this report is only a small step towards the process it helps to determine and document the outcomes, difficulties and considerations when using the treatments considered.

2. Methodology

2.1. Sample procurement

To acquire the data for the study, 12 female Sprague-Dawley rats were raised in identical environmental conditions (diet, temperature and humidity). The rats were randomly divided into 4 groups, to which were applied a specific medical treatment according to the weight of the animal. This study is divided into three phases, where each phase consists of 4 rats. The phases follow each other chronologically in 3-month intervals. The samples are thus harvested every 3 months. A rat provides two bone samples: its left and right femur, which is then prepared and conserved for biomechanical testing. The rats undergo a surgical procedure at approximately 6 months of age. The average age of a Sprague Dawley rat is around 2.5-3.5 years [6], at 6 months the animals have reached maturity. At the end of the 12-week treatment period, each rat was sacrificed for bone extraction. The samples of this study have been separated into four different groups: normal fracture, control group, “A” treatment and “B” treatment (Table 1).

Table 1. Sample group characterization

Sample Group Description	Label	Group Name
Normal fracture with physiological serum	F+S	Normal fracture
Subtraction osteotomy with physiological serum	OS+S	Control group
Subtraction osteotomy with “B” treatment	OS+B	“B” treatment
Subtraction osteotomy with “A” treatment	OS+A	“A” treatment

The physiological serum acts as a placebo for the normal fracture and control group, whilst providing the animals with the required nutrients. The operation procedure was the same for the OS+S, OS+A and OS+B sample groups. The surgical procedure and theoretical bone healing progression has been summarized in the sketch of Figure 1. The operation of F+S samples was similar except that there was no bone subtraction and thus no gap, as it is a simple fracture. In the operation, the rat’s skin was incised and a 2 mm section from the centre of the femur was removed, (subtraction osteotomy). Once the gap was created a stainless steel screw (2mm x 24mm) was inserted in the lower extremity of the right femur to maintain the gap. To verify that the callus was developing correctly, the animals were monitored taking x-rays of the right femurs (Figure 2: 7 days after the operation, 6 weeks after start the treatment and 12 weeks prior to the slaughter). The pictures were analized to measure the gap size (in mm) and evolution throughout the treatment. In order to conduct the biomechanical tests on the bones, they were removed from the rats by surgical procedure carried out by medical personnel. The extracted bones were conserved to avoid their deterioration through drying, in a saline solution (HBSS) at 4ºC until they were tested.

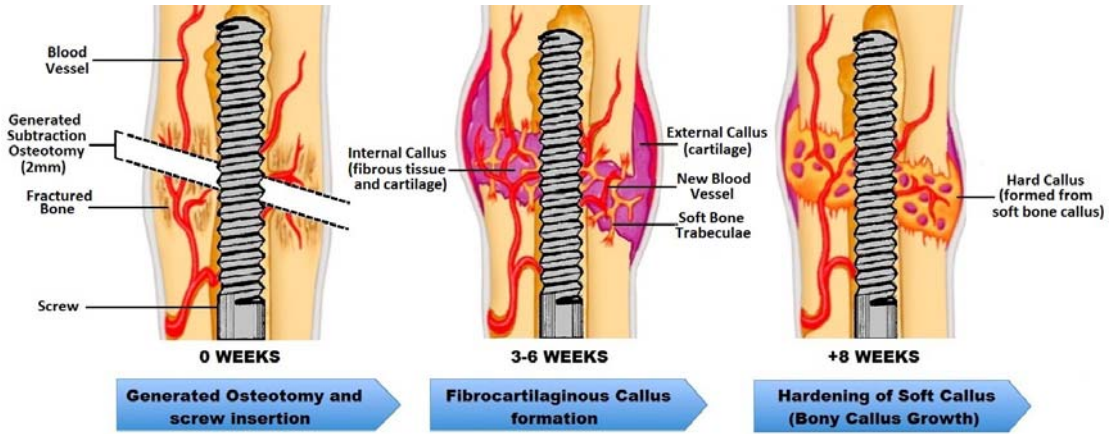

Figure 1. Sketch of the fracture healing progress throughout the study [1]

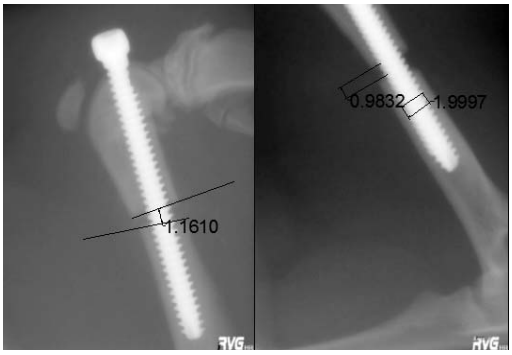

Figure 2. Gap measurement and scale verification

2.2 Four Point Bending Test (4PBT)

The bones were cleaned to remove any excess of cartilage or ligaments. Figure 3a shows the process by using a saw, a mechanical clamp and protective wrapping, to prevent any damage to the sample. Once the bone extremities had been removed (Figure 3b) they were conserved for UMI testing.

a) 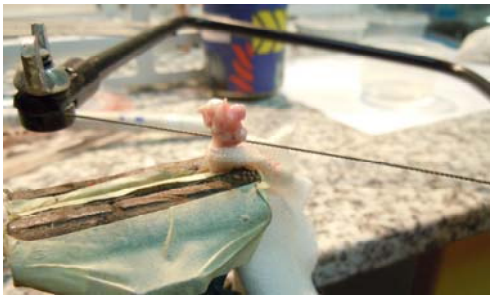

b) 

Figure 3. a) Removal of bone upper extremity during sample preparation and b) final aspect

The samples were tested within 24 hours of the bone extraction to obtain the most accurate results possible. Before each test the bones were preheated to 37ºC in a saline solution to replicate the temperature in the bone's usual environment. 4PBTs were carried out on the diaphysis (shaft of the bone) using an universal testing machine (0.5 class). The sample was placed within a methacrylate container, and a water bath was set to 37°C. A pump was then positioned so that the heated serum could flow around the sample, thus recreating the in vivo conditions. Figure 4a displays the main elements of the installation.

In biomechanics, 4PBTs are important as they allow the application of a bending load to a bone shaft sample, which is generally how mid-shaft femur fractures occur [7]. During the 4PBTs the loading force was exerted by a hydraulic piston, through two points namely two cylindrical steel rods. The sample received this load whilst being laid between two cylindrical rods at 15mm apart. The load rate was 10 mm/min until the two points of the hydraulic arm reached the centre of the sample surface. Figure 4b shows the hydraulic actuator before it has reached the sample. F represents the force exerted by the hydraulic arm. In a 4PBT bone samples act as beams, the upper part of the bone being in compression and the lower part in tension. During the tests, the force-displacement graphs were obtained by collecting the numerical data obtained from the machine. These graphs enabled the determination of three mechanical properties: maximum force (F_{max}), energy absorbed up to the maximum force (E_a) and rigidity which are represented in the typical force-displacement curve obtained during a 4PBT shown in Figure 5.

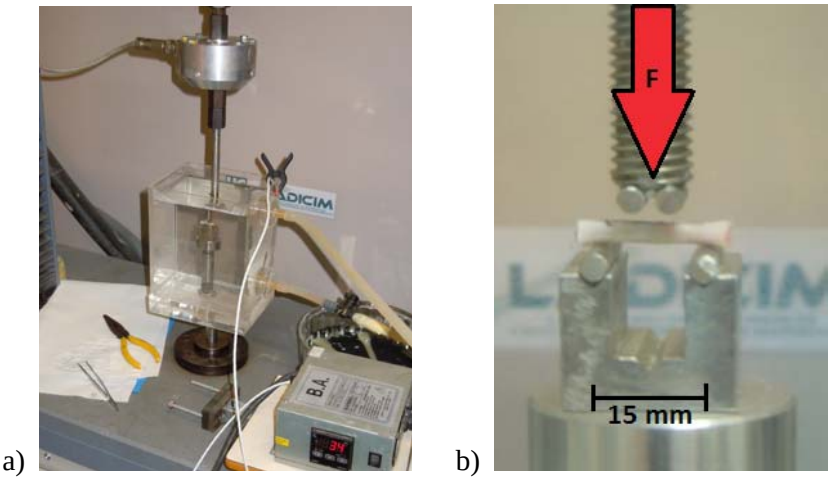

Figure 4. a) Four point bending test setup and b) Detail of bone sample about to be loaded for a 4PBT

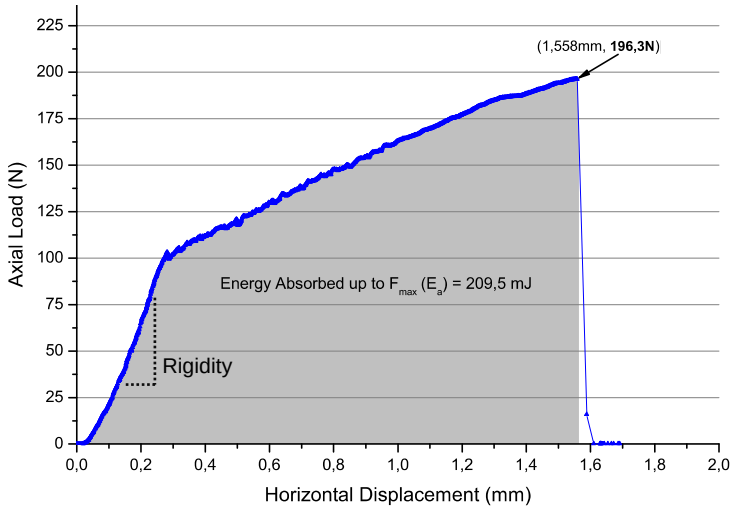

Figure 5. Typical force-displacement curve of a 4PBT

2.3 Ultra-Micro Indentation Test (UMI)

The second experiment undertaken on the samples was the UMI test, enabling the extraction of hardness [8-9] and elastic modulus parameters from the samples. The cut bone extremities were

embedded in a two-component acrylic (see Figure 6a) to provide the samples with a support that can then be used to polish the surface using an automatic grinder (see Figure 6b). The grinder holds down the sample, using suction cups, onto rotating (150 rpm) polishing plates to smooth the surface. The machine uses water as a lubricant. The polishing process is gradual being the carbide papers of the following grain sizes: 500, 1200, 2400 and 4000. Finally, a velvet disc was used to provide a smooth finish to the samples before they were tested (see Figure 6c).

a) 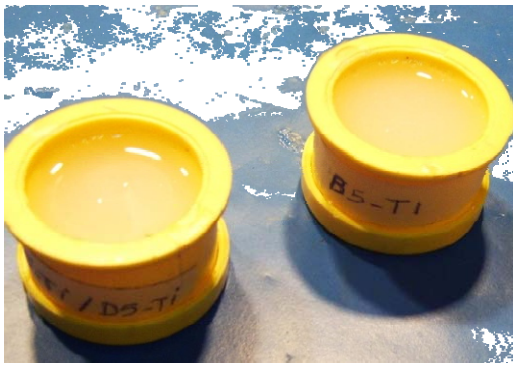 b)  c) 

Figure 6. a) Embedding bone extremities in resin. b) polishing machine. c) polished bones

Once the samples were polished, they were stored in a saline solution at 5°C to avoid the exposed polished surface from deteriorating. Prior to test the samples were preheated to 37°C in a controlled saline solution bath to recreate in vivo conditions. The UMI tests were carried out using a Shimadzu DUH-211 with a pyramidal Berkovich indenter tip (see Figure 7a and 7b). The test consists of two main phases, loading up to 150 mN and then discharging. Each phase is followed by a holding period: 10 seconds for the loading and 5 seconds for the discharge. The loading and unloading rate was 2,6648 mN/sec. On each sample, both the trabecular and cortical tissues were analyzed. For each area 14 indentations were made in order to obtain the hardness and elastic modulus. The hardness calculated is defined as the ratio between the force applied by the indenter and the area left after the indentation (see Figure 7c).

a) 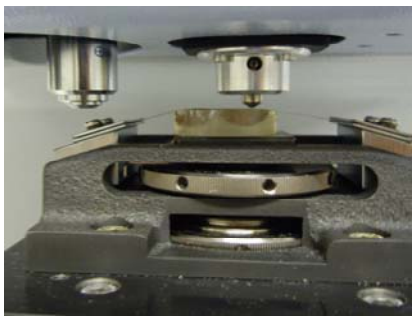 b) 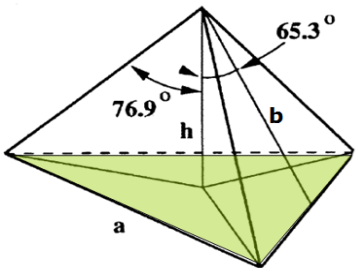

c) 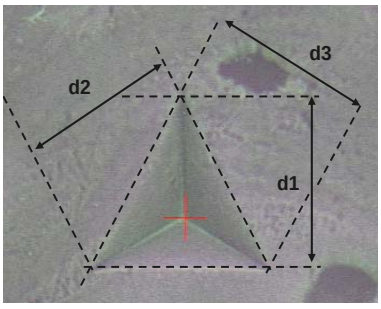

Figure 7. UMI test description. a) Machine. b) indenter tip geometry. c) projected area

A typical UMI graph is shown in Figure 8. The loading and discharge phases are clearly visible and h_f, h_r, h_s, h_c and h_m all represent specific indentation depths that occur during the test. The dashed line, with a slope S, is used to calculate the indentation elastic modulus. It intersects the x-axis at the depth h_r. Once the data was collected it was analyzed using variety of statistical tools.

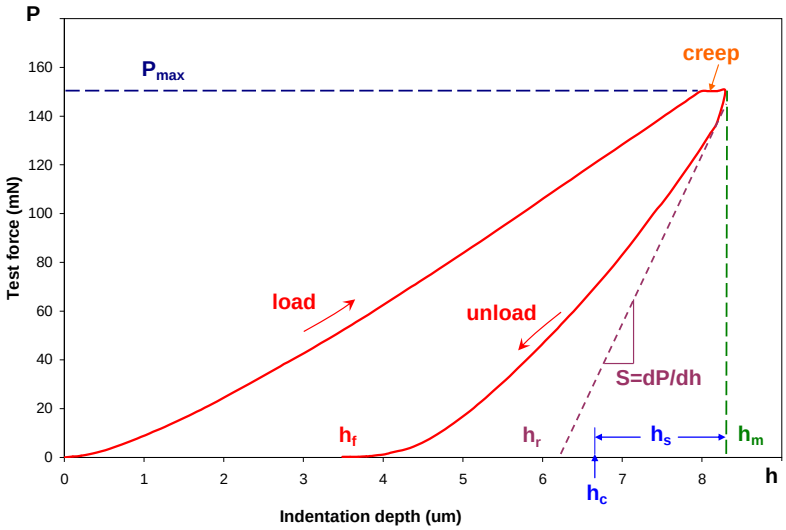

Figure 8. Typical UMI graph of force against indentation depth

3. Results and Discussion

3.1 Four Point Bending Tests

3.1.1 Maximum Force

Figure 9 shows the F_{max} values obtained. Above each sample group is the average, followed by the standard deviation and its line of proportional length. For ease of comparison, the maximum forces of both left and right femur have been included on the figure.

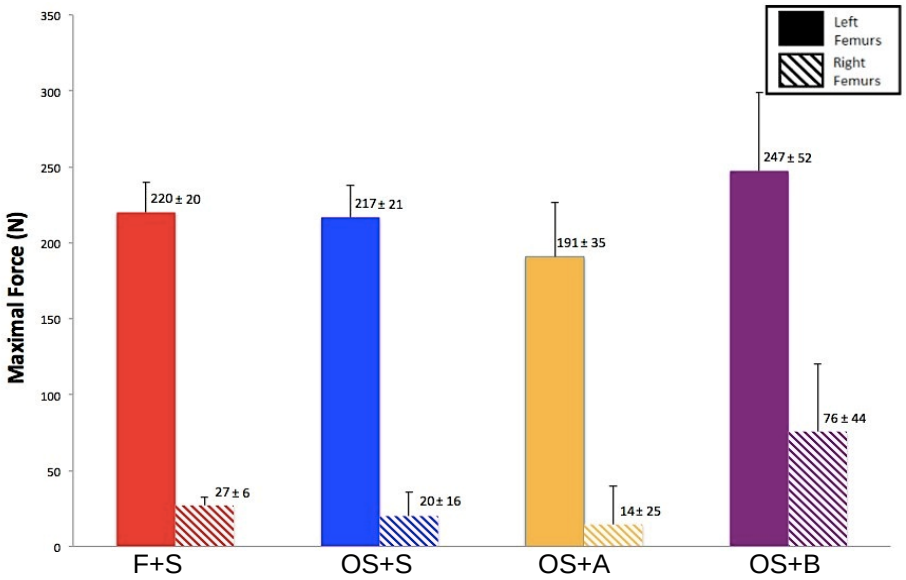

Figure 9. Bar chart displaying maximum force values and variation for each treatment

The relationship between the gap size and F_{max} confirms the effectiveness of “B” treatment over “A” treatment. Using the gap sizes (measured on the x-rays) and the F_{max} values above, the relationship between the gap size and F_{max} can be plotted using power trend lines (Figure 10).

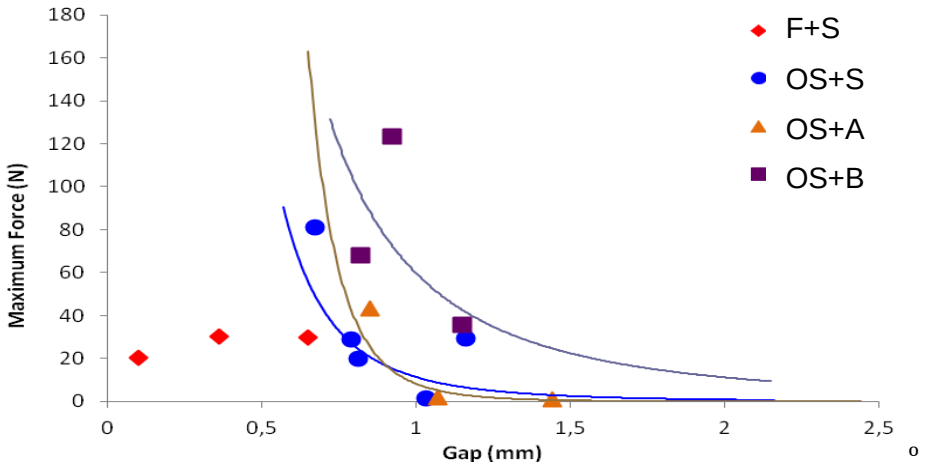

Figure 10. Relationship between F_{max} and gap size

In Figures 9 and 10, the patterns are clear in terms of the effectiveness of the treatments. Above a certain gap size (Figure 10) the "B" treatment is more effective than the "A" treatment; as for the same gap the samples require a higher F_{max}.

3.1.2 Energy Stored up to Maximum Force

The energy absorbed up to the point of maximum force (E_a) can be seen in the bar chart of Figure 11. Above each bar is the average energy absorbed and variation (standard deviation) represented numerically and by a line of proportional length.

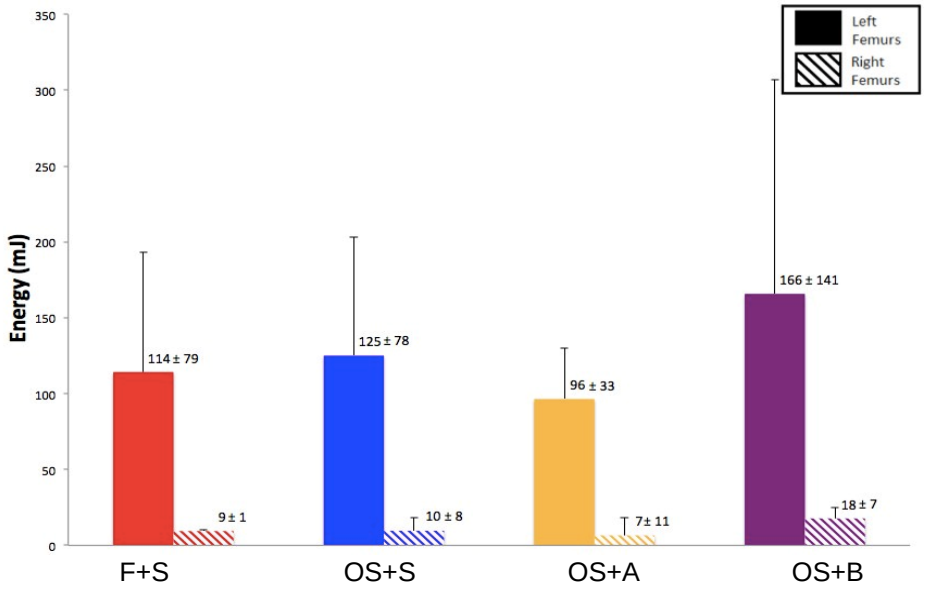

Figure 11. Energy absorbed up to maximum force

3.1.3 Rigidity

The rigidity of the samples obtained from the force-displacement curves are shown in the scatter point diagram of Figure 12. Both left and right femur data have been placed on the diagram to facilitate comparison. The average rigidity is indicated alongside the data points of each group.

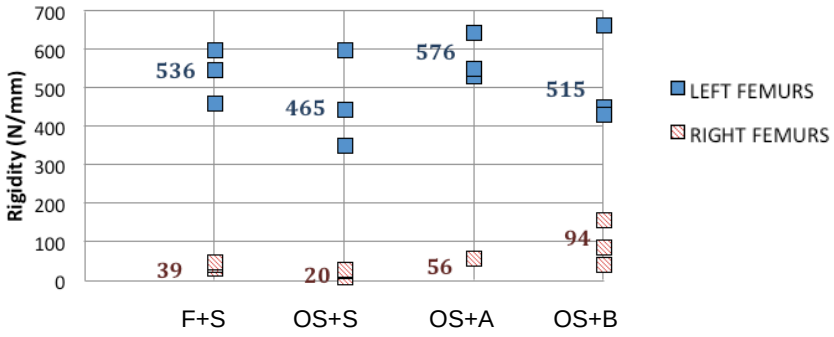

Figure 12. Scatter plot diagram of rigidity values for each sample

The values obtained for rigidity vary substantially, although there does appear to be a trend. The pattern is more evident in the right femurs, where the effect is more acute due to the subtraction osteotomy. The rigidity of the normal fracture is considerably higher than that of the subtraction osteotomy for left and right femurs. These results are expected, as a normal fracture should be more rigid than a bone that has undergone a surgical procedure (subtraction osteotomy).

3.2 Ultra-Micro Indentation Tests

3.2.1 Cortical and Trabecular Hardness

UMI tests were carried out to measure cortical and trabecular hardness. Both of the two types of tissue must be represented separately as they have different biological structure. To enable a clearer understanding Figure 13 shows the areas analyzed on the bones. There is a box plot diagram for each of the four groups, enabling a comparison of the data obtained for the same area of different samples.

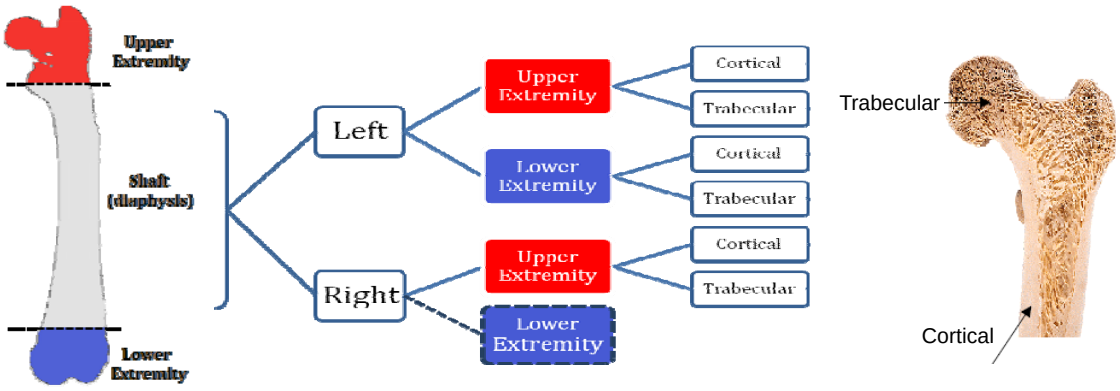

Figure 13. Diagram schematising the various areas used for hardness testing

As an example Figure 14 presents the hardness of one area depicted in Figure 13. The boxes represent the interquartile ranges (25 and 75%), the horizontal line the median and the unfilled square the mean. The whiskers are outliers. Crosses indicate the minimum and maximum points. To compare the treatments to the control group a two-sample t-test was used. The null hypothesis of this test is that the means of the two groups compared are equal. Using a level of 0.05, if the p parameter is lower than 0.05, the two sample groups compared are significantly different.

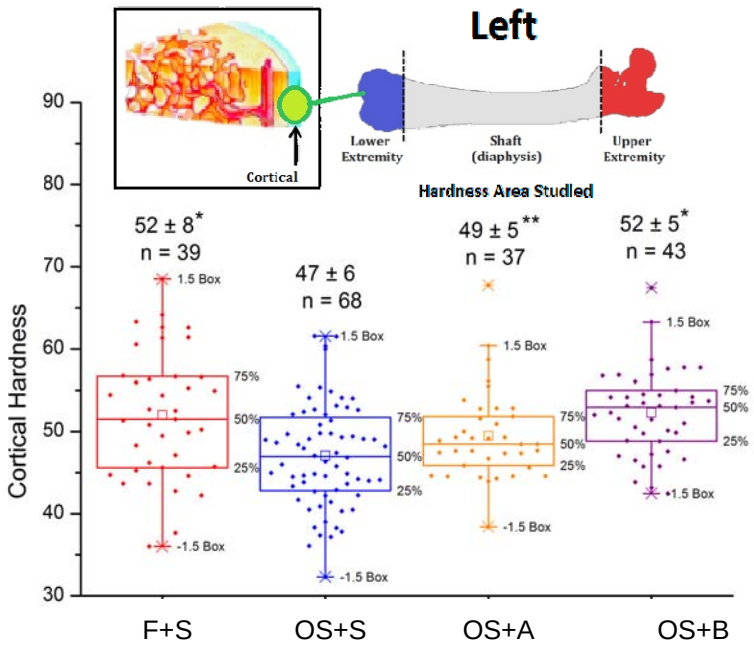

Figure 14 - Cortical hardness for the lower extremities of left femurs.
*p<0.01 for OS+S vs. F+S and OS+S vs. OS+B. **P~0.05 for OS+S vs. OS+A.

3.2.2 Elastic Modulus

The indentation elastic moduli of the left femurs are similar. Figure 15 shows the values of the right femurs and there is an obvious difference between the four groups. The cortical elastic modulus of the control group (OS+S) is lower than that of each of the treatments. In the operated bones the medical treatments increase the cortical elastic modulus to the values of a normal fracture.

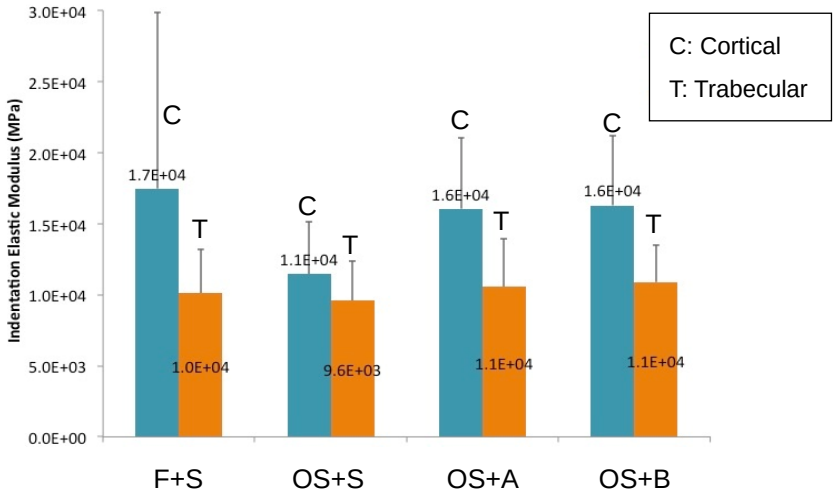

Figure 15 - Bar chart of indentation elastic modulus for right femurs

4. Conclusions

- Traditional techniques used to characterize the mechanical behavior of engineering materials can successfully be applied to biological materials. The methods used enable the comparison of the effects of the medical treatments on the mechanical properties of the material studied.

- 4PB tests results show that “B” treatment provides the highest results relating to callus resistance, toughness and rigidity. The relationship between the maximum force and the gap size for the right femurs also shows that B treatment is above that of the “A” treatment.

Treatment	F_{max} (N)	E_a (mJoule)	Rigidity ($N \cdot mm^{-1}$)
“A” (right femurs)	14	7	56
“B” (right femurs)	76	18	94

- UMI tests results show that cortical tissue is consistently harder than the trabecular bone. In both cases “B” treatment provides harder samples and is thus more effective.

Treatment	Cortical Hardness (GPa)	Trabecular Hardness (GPa)
“A” (right femurs)	0,61 ± 0,08	0,54 ± 0,05
“B” (right femurs)	0,67 ± 0,1	0,57 ± 0,06

“A” and “B” treatments provide, especially in the right operated femurs, an elastic modulus equal to that of a normal fracture.

- Examining the bone fracture healing of rat femurs in a pseudoarthrosis model, “B” treatment provides pathological bones with more suitable biomechanical properties than “A” treatment.

Acknowledgements

The authors of this work would like to express their gratitude to IFIMAV (Institute of formation and Investigation Marqués de Valdecilla) for the economical support to perform the study.

References

[1] P. Siegel. ANAT 416: Development, Disease and Regeneration, Lecture: Bone Remodelling and Fracture Repair. [Class handout]. Retrieved March 5, 2012.
[2] F. H. Netter. Musculoskeletal system: Anatomy, physiology, and metabolic disorders. Summit, New Jersey: Ciba-Geigy (1987).
[3] A. G. Robling, A. B. Castillo & C. H. Turner. Biomechanical and Molecular Regulation of Bone Remodeling. The Annual Review of Biomedical Engineering, vol. 8, (2006) 455–498.
[4] V. C. Mow & W. M. Lai. Mechanics of Animal Joints. Annual Review of Fluid Mechanics, vol. 11, p. 247. Retrieved March 28, 2012
[5] C. H. Turner & D. B. Burr. Basic biomechanical measure of a bone: a tutorial. Bone, vol. 14, (1993) 595–608.
[6] Sprague Dawley. (2001, January 31). Retrieved March 03, 2012, from http://www.sageresearchmodels.com/research-models/outbred-rats/sprague-dawley
[7] A. I. King. Fundamentals of Impact Biomechanics: Part 2. Biomechanics of the Abdomen, Pelvis, and Lower Extremities. Annual review of Biomedical Engineering, 3, (2011) 27–55.
[8] S. L., Ferreri, B. Hu & Y. Qin. Nano indentation Measurements of Viscoelastic Materials Properties are sensitive to Preparation Techniques. *Bioengineering Conference,* Proceedings of the 2010 IEEE 36th Annual Northeast. Stony Brook, New York: Stony Brook University.
[9] L. Sun et al. Evaluation of the mechanical properties of rat bone under simulated microgravity using nanoindentation. Acta Biomaterialia, vol. 5 (9) 2009.